ELSEVIER

Journal of Alloys and Compounds 434–435 (2007) 424–427

Journal of ALLOYS AND COMPOUNDS

www.elsevier.com/locate/jallcom

High temperature behavior of ball-milled Al–Ni–Ce–Co alloys

A. Révész *, P. Henits, Zs. Kovács

Department of Materials Physics, Eötvös University at Budapest, P.O.B. 32, Budapest H-1518, Hungary

Available online 4 October 2006

Abstract

Microstructure of ball-milled $Al_{85}Ni_8Ce_5Co_2$ powder indicates the formation of fine nanoparticles with some amorphous fraction. Thermal analysis revealed that the release of internal stress and grain growth is followed by the redistribution and possible melting of high solute concentration interfaces. In addition, mechanical properties of compacted powder specimens were also investigated.

Keywords: Mechanical alloying; Thermal analysis; Nanostructured materials; X-ray diffraction

1. Introduction

Conventional aluminum alloys have been well known for their use as light-weight components in engineering applications, particularly in the aerospace industry, for some time. Recently, non-equilibrium Al-based alloys with Al-content above 80 at.% have received great attention since they exhibit advantageous mechanical properties, with high tensile strength and good ductility [1–4], hardness [5], wear [6] and corrosion resistance [7]. Nevertheless, the low thermal stability of these materials still limits their wide-spread technological applications. Typically, such alloys are prepared by rapid quenching, however, alternatively, they are also produced mechanical alloying or ball milling (BM) [8,9]. These techniques can easily be combined with suitable powder compaction, promise to allow preparation of bulk specimens with much larger dimensions than those available through rapid quenching. The amorphous or crystalline nature of numerous Al–TM–RE ternary alloy systems was reviewed [10,11].

In this paper we report on the formation and high temperature behavior of ball-milled nanocrystalline $Al_{85}Ni_8Ce_5Co_2$ alloys. Additionally, microstructural and mechanical properties were studied on compacted specimens.

2. Experimental

Nanocrystalline $Al_{85}Ni_8Ce_5Co_2$ powders were mechanically alloyed in a vibratory mill under high vacuum for milling times of 4, 48, 100 and 192 h, respectively. The as-milled powders were then compacted into small pellets under a uniaxial load of 1 GPa.

Microstructures were examined by powder X-ray diffraction (XRD) on a Philips Xpert diffractometer using Cu Kα radiation in θ–2θ geometry. Transmission electron microscopy (TEM) images and selected area electron diffraction (SAED) patterns were taken by a JEOL 2000 microscope operating at 200 keV. Samples for TEM studies were prepared by electropolishing.

Thermal stability experiments were carried out in a Perkin-Elmer power compensated calorimeter (DSC) under pure dynamic argon atmosphere. Continuous heating measurements were performed at 20 K min^{-1}. High temperature measurements were performed on a Setaram differential thermal analyzer (DTA) equipment to study the melting behavior. The melting point was determined as the intercept of the calorimetric baseline and the straight line fitted to the leading edge of the endotherm peak.

Microhardness (HV) testing was performed on polished compacts using a Shimandzu DUH-202 dynamic depth sensing microhardness tester with a Vickers indenter at a load rate of 7 mN/s up to 200 mN. The values of HV were determined by averaging 10 indents.

3. Results and discussion

Fig. 1 shows the bright field TEM images and the corresponding SAED patterns of the $Al_{85}Ni_8Ce_5Co_2$ powders. As it is seen, 4 h of BM results in the formation of submicrometer particles with an average grain size of about 50–100 nm. With increasing milling time the average grain size decreases, while a featureless background forms. The characteristic size of the dark spots in Fig. 1d is about 10–20 nm.

The sharp rings with white spots on the SAED pattern of the sample milled for 4 h correspond to fcc-Al. Afterwards the rings become broaden while the intensity of the white diffraction spots decrease confirming a nanocrystallization process. Moreover, in Fig. 1d a diffuse halo can also be seen that corresponds to an amorphous background, thus the final microstructure can be

* Corresponding author. Tel.: +36 1 372 2823; fax: +36 1 372 2811.
E-mail address: reveszadam@ludens.elte.hu (A. Révész).

0925-8388/$ – see front matter © 2006 Elsevier B.V. All rights reserved.
doi:10.1016/j.jallcom.2006.08.160

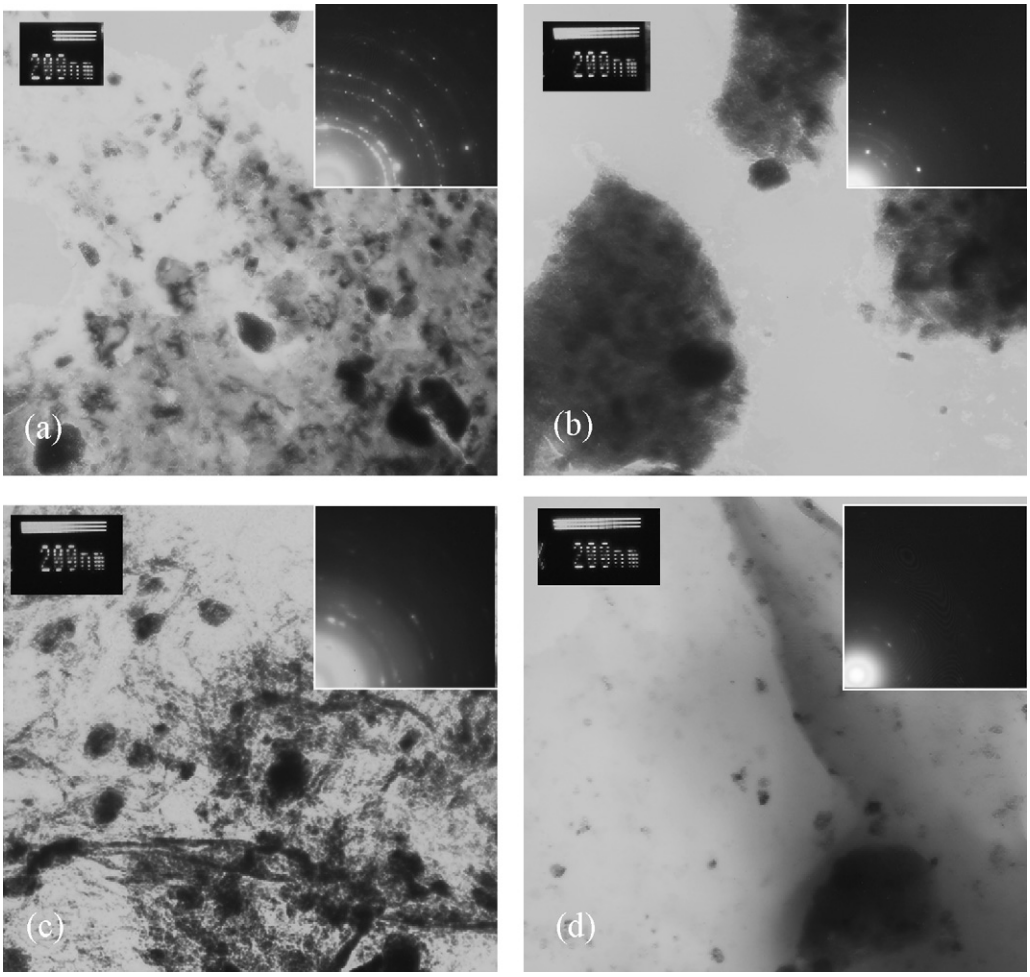

Fig. 1. Bright field transmission electronmicroscopy images and corresponding selected area diffraction patterns of $Al_{85}Ni_8Ce_5Co_2$ powders milled for (a) 4 h, (b) 48 h, (c) 100 h and (d) 192 h.

considered as a nanocomposite with some amorphous fraction on a submicrometer scale.

The evolution of the volume average grain size through the BM process was determined from X-ray diffraction line broadening. The well-known Scherrer equation [12] was applied for the (1 1 1) fcc-Al peak since there is no overlap with other diffraction peaks (see the inset in Fig. 2). As it can be seen from Fig. 2 the grain-size values decrease rapidly at the initial stage of ball-milling and afterwards the rate of the grain refinement continuously decreases reaching a minimum value of 13 nm after 192 h of BM. This value is remarkably smaller than that reported for ball-milled pure Al [13].

The thermal behavior of the powders was examined by DSC as shown in Fig. 3. Each curve exhibits a broad exothermal heat contribution at around 550 K followed by an endothermic peak in the range of 650–750 K. The alloys milled for longer times (100 and 192 h) reveal a small exothermic pre-peak at around 390 K. Generally, the area of the exothermic peak was found to increase with prolonged BM time.

The high temperature behavior of the $Al_{85}Ni_8Ce_5Co_2$ powders was systematically studied by DTA during heating and cooling. The thermogram exhibits an endothermic contribution corresponding to the melting of pure Al (T_m) at 871 K for the powder milled for 192 h (see Fig. 4). From the area of the melting endotherm, the relative mass fraction of the unreacted pure elemental Al was found to be 8%. At higher temperatures (T_p = 968 K) an exothermic reaction occurs with a released enthalpy of 164 J g^{-1} followed by several smaller melt-

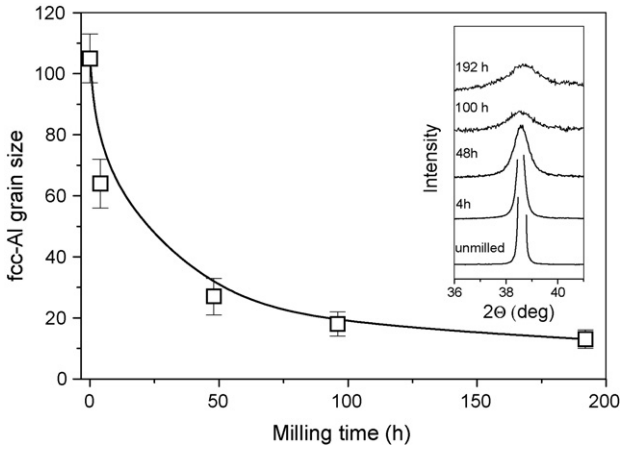

Fig. 2. Average fcc-Al grain size vs. milling time. The inset shows the line broadening of the (1 1 1) Al Bragg-peak.

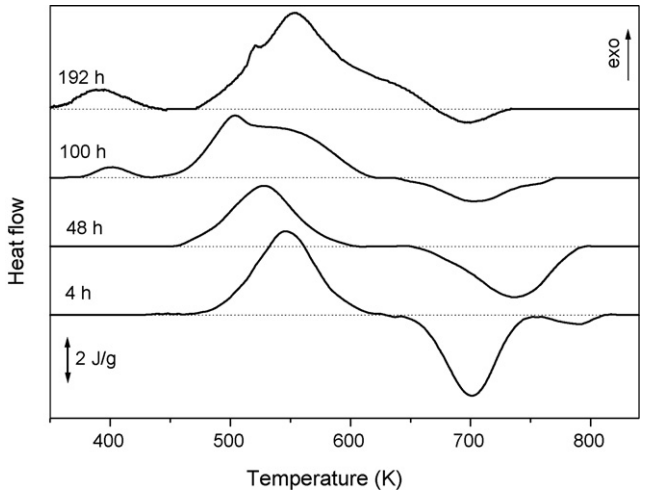

Fig. 3. Differential scanning calorimetry curves obtained at heating rate of 20 K min^{-1} for different milling times.

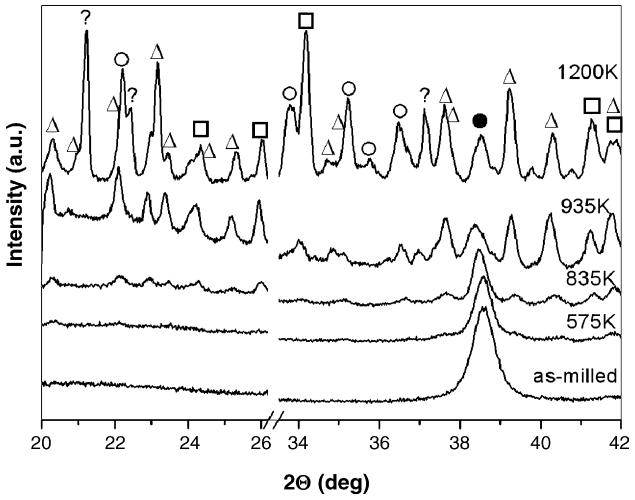

Fig. 5. X-ray diffraction patterns of the 48 h powder obtained after linear heating to different temperatures. The symbols ●, □, △, ◯ and ? denotes the Bragg-peaks of fcc-Al, Al_3Ni, Al_9Co_2, Al_4Ce and an unidentified phase, respectively.

ing endotherms. The inset in Fig. 4 shows that with increasing BM time the onset of T_m shifted to lower temperatures in accordance with the melting behavior of small nanoclusters following the predicted inverse grain-size dependence [14]. On the other hand, it was found that T_p increases with increasing BM time.

In order to study the microstructure at different temperatures, the powder milled for 48 h was continuously heated up to 575, 835, 935 and 1200 K, respectively. In Fig. 5 the XRD patterns show that the width of the (1 1 1) fcc-Al peak decreases slightly, when the samples is heated above the first exothermic peak (575 K), corresponding to a moderate grain growth from 27 to 36 nm. Consequently, the area of the exothermic peak can be associated with a released enthalpy corresponding to grain coarsening and annihilation of internal strain.

At 835 K, above the first broad endothermal peak, some faint Bragg peaks of several intermetallic phases, i.e. Al_9Co_2, Al_4Ce, Al_3Ni appear, while the intensity of the fcc-Al peaks does not change significantly. In our opinion this heat effect can be ascribed as the redistribution of high solute concentration inter-

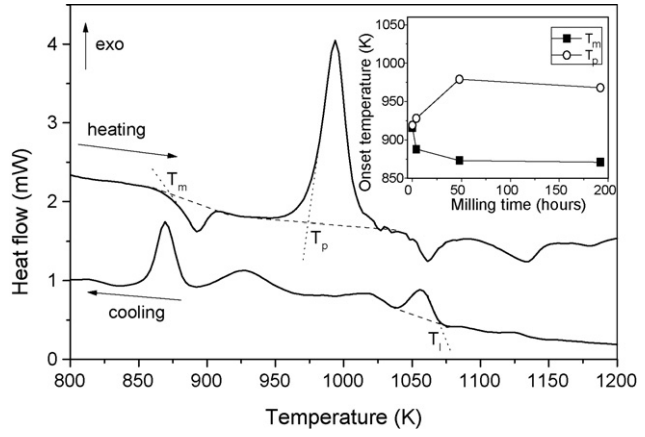

Fig. 4. High temperature differential thermal analysis curve for the powder milled for 192 h. T_m and T_p correspond to the onset of the Al-melting and to the onset of the growth of the intermetallic phases, respectively. The inset shows the variation of T_m and T_p vs. milling time.

faces (surface melting). Simultaneously, the Al-grains grow up to 42 nm.

Linear heating above the Al-melting peak (935 K) results in a more dominant appearance of the Al_9Co_2, Al_4Ce and Al_3Ni Bragg-peaks, however, melting and refreezing does not result in the complete elimination of elemental Al. At 1200 K, above the high temperature exothermic peak, the relative intensity of the Al_4Ce and Al_3Ni Bragg-peaks increase drastically and simultaneously an unidentified phase also appears.

Practically, at above 935 K the molten Al causes the formation of faster percolation channels, accordingly enhance the diffusion of Ce, Ni and Co in Al. Above the Al-melting temperature,

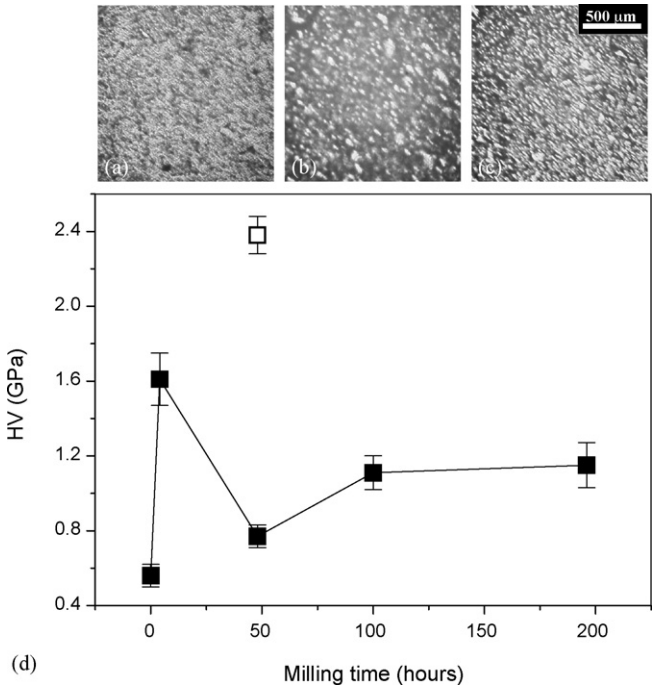

Fig. 6. Optical microgrpahs of $Al_{85}Ni_8Ce_5Co_2$ powders milled for (a) 4 h, (b) 48 h, (c) 192 h and (d) microhardness values vs. milling time.

the liquid Al in huge volume promotes the growth of the intermetallic phases. This effect can be associated with the sharp exothermic peak on the DTA signal (see Fig. 4). At shorter BM times, the difference between T_m and T_p is just a few degrees (see the inset in Fig. 4) indicating that the growth of Al_9Co_2, Al_4Ce and Al_3Ni starts immediately just after the liquid Al forms. At longer BM times when the average grain size is smaller, T_m increases due to the restricted diffusion corresponding to the enhanced density of interfaces.

Fig. 6 summarizes the optical micrographs and mechanical properties of the compacts. The 4 h alloy exhibit a homogeneous morphology on micron scale, however, in the case of the sample milled for 48 h two distinct regions appears on a 100 μm scale. Prolonged milling up to 192 h results in a remarkable fragmentation.

The microhardness of the 4 h powder-compact is three times higher than that of the compact of unmilled mixture. After 48 h of BM the two distinct regions shows separate values of 0.8 and 2.4 GPa, respectively. After longer milling the HV values belong to the average hardness of the two measured areas.

4. Conclusions

Ball-milling of $Al_{85}Ni_8Ce_5Co_2$ powders results in the formation of fine nanoparticles with some amorphous fraction. Combination of DSC, DTA and XRD experiments revealed that release of internal stress and grain growth is followed by the redistribution and possible melting of high solute concentration interfaces. In the case of shorter milling times, the growth of Al_9Co_2, Al_4Ce and Al_3Ni starts immediately after the liquid Al forms. Progressive milling results in the separation of T_m and T_p.

Acknowledgements

Zs. K. is grateful for the support of the Postdoctoral Research Program (D048461) of the Hungarian Scientific Research Fund. The work has partially been supported by the Hungarian Scientific Research Fund (OTKA) under grants T-043247 and T-046990.

References

[1] Y. He, S.J. Pooh, G.J. Shiflet, Science 241 (1988) 1640.
[2] A. Inoue, K. Ohtera, A.P. Tsai, T. Masumoto, Jpn. J. Appl. Phys. 27 (1988) L289.
[3] K. Ohtera, A. Inoue, T. Terabayashi, H. Nagahama, T. Masumoto, Mater. Trans. JIM 33 (1992) 77.
[4] A. Inoue, Y. Horio, Y.H. Kim, T. Masumoto, Mater. Trans. JIM 33 (1992) 669.
[5] Z.C. Zhong, X.Y. Jiang, A.L. Greer, Mater. Sci. Eng. A226–228 (1997) 531.
[6] T. Gloriant, A.L. Greer, Nanostruct. Mater. 10 (1998) 389.
[7] F. Audebert, S. Vázquez, A. Gutiérrez, I. Vergara, G. Álvarez, A. Garcia Escorial, H. Sirkin, Mater. Sci. Forum 269–272 (1998) 837.
[8] I. Börner, J. Eckert, Scripta Mater. 45 (2001) 237.
[9] G.M. Dougherty, G.J. Shiflet, S.J. Poon, Acta Metal. Mater. 42 (1994) 2275.
[10] Nonequilibrium Phase Diagrams of Ternary Amorphous Alloys, in: J.-Z. Yu, A.-P. Tsai, T. Masumoto (Eds.), Landolt-Börnstein, New Series, vol. III/37A, Springer-Verlag, Berlin, Germany, 1997.
[11] Á. Révész, L.K. Varga, P.M. Nagy, J. Lendvai, I. Bakonyi, Mater. Sci. Eng. A 351 (2003) 160.
[12] H.P. Klug, L.E. Alexander, X-ray Diffraction Procedures for Polycrystalline and Amorphous Materials, Wiley, New York, USA, 1974.
[13] Á. Révész, J. Mater. Sci. 40 (2005) 1643.
[14] P.R. Chouchman, W.A. Jesser, Philos. Mag. Lett. 35 (1977) 223.